

AD-A061 686

AEROSPACE CORP EL SEGUNDO CALIF IVAN A GETTING LABS

F/6 7/4

TEMPERATURE DEPENDENCE OF HE(V SUB 1 = 1) + HF(V SUB 2 = 0) VIB--ETC(U)

AUG 78 R L WILKINS, M A KWOK

F04701-77-C-0078

UNCLASSIFIED

TR-0078(3603)-5

SAMSO-TR-78-76

NL

| of |  
AD  
A061 686



END  
DATE  
FILMED  
2-79  
DDC

**LEVEL II**

12

SC

AD A061686

DDC FILE COPY

**Temperature Dependence of HF( $v_1 = 1$ ) + HF( $v_2 = 0$ )  
Vibrational Relaxation**

R. L. WILKINS and M. A. KWOK  
Aerophysics Laboratory  
The Ivan A. Getting Laboratories  
The Aerospace Corporation  
El Segundo, Calif. 90245

15 August 1978

Interim Report

APPROVED FOR PUBLIC RELEASE;  
DISTRIBUTION UNLIMITED

DDC  
RECEIVED  
NOV 30 1978  
D

Prepared for  
AIR FORCE WEAPONS LABORATORY  
Kirtland Air Force Base, N. Mex. 87117

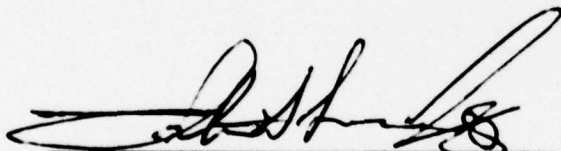
SPACE AND MISSILE SYSTEMS ORGANIZATION  
AIR FORCE SYSTEMS COMMAND  
Los Angeles Air Force Station  
P.O. Box 92960, Worldway Postal Center  
Los Angeles, Calif. 90009

78 11 13 084

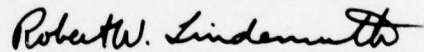
This interim report was submitted by The Aerospace Corporation, El Segundo, CA 90245, under Contract No. F04701-77-C-0078 with the Space and Missile Systems Organization, Deputy for Advanced Space Programs, P. O. Box 92960, Worldway Postal Center, Los Angeles, CA 90009. It was reviewed and approved for The Aerospace Corporation by W. R. Warren, Jr., Director, Aerophysics Laboratory. Lieutenant Arturo G. Fernandez, SAMSO/YCPT, was the project officer for Advanced Space Programs.

This report has been reviewed by the Information Office (OI) and is releasable to the National Technical Information Service (NTIS). At NTIS, it will be available to the general public, including foreign nations.

This technical report has been reviewed and is approved for publication. Publication of this report does not constitute Air Force approval of the report's findings or conclusions. It is published only for the exchange and stimulation of ideas.



Arturo G. Fernandez, Lt, USAF  
Project Officer



Robert W. Lindemuth, Lt Col, USAF  
Chief, Technology Plans Division

FOR THE COMMANDER



LEONARD E. BALTZELL, Col, USAF  
Asst. Deputy for Advanced  
Space Programs

UNCLASSIFIED

SECURITY CLASSIFICATION OF THIS PAGE (When Data Entered)

19 REPORT DOCUMENTATION PAGE		READ INSTRUCTIONS BEFORE COMPLETING FORM
18 1. REPORT NUMBER SAMSOTR-78-76	2. GOVT ACCESSION NO.	3. RECIPIENT'S CATALOG NUMBER
6 4. TITLE (and Subtitle) TEMPERATURE DEPENDENCE OF HF( $v_1 = 1$ ) + HF( $v_1 = 0$ ) VIBRATIONAL RELAXATION	7. AUTHOR(s) Roger L. Wilkins <del>and</del> Munson A. Kwok	8. TYPE OF REPORT & PERIOD COVERED Interim rept.
Sub 1	Sub 2	9. PERFORMING ORG. REPORT NUMBER TR-0078(3603)-5
10		10. CONTRACT OR GRANT NUMBER(s) F44701-77-C-0078
9. PERFORMING ORGANIZATION NAME AND ADDRESS The Aerospace Corporation El Segundo, Calif. 90245		10. PROGRAM ELEMENT, PROJECT, TASK AREA & WORK UNIT NUMBERS
11. CONTROLLING OFFICE NAME AND ADDRESS Air Force Weapons Laboratory Kirtland Air Force Base, N. Mex. 87117		11. REPORT DATE 15 August 1978
14. MONITORING AGENCY NAME & ADDRESS (if different from Controlling Office) Space and Missile Systems Organization Air Force Systems Command Los Angeles, Calif. 90009		12. NUMBER OF PAGES 30
16. DISTRIBUTION STATEMENT (of this Report) Approved for public release; distribution unlimited.		13. SECURITY CLASS. (of this report) Unclassified
		15. DECLASSIFICATION/DOWNGRADING SCHEDULE
17. DISTRIBUTION STATEMENT (of the abstract entered in Block 20, if different from Report)		12) 39 p.
18. SUPPLEMENTARY NOTES		
19. KEY WORDS (Continue on reverse side if necessary and identify by block number) Chemical Kinetics Energy Transfer Hydrogen Fluoride	Rate Coefficients Rotational Relaxation Vibrational Relaxation	
20. ABSTRACT (Continue on reverse side if necessary and identify by block number) A kinetics model of infrared laser-induced fluorescence experiments has been used to simulate the experimental quenching rate coefficients reported between 300 and 4000 K for the vibrational relaxation of HF( $v_1 = 1$ ) by HF. This rotational nonequilibrium model is based on the predicted energy-transfer mechanisms in hydrogen fluoride systems reported in a trajectory study by Wilkins. This model includes $v \rightarrow R$ , $R \rightarrow v$ , $R \rightarrow (R', T')$ , and $(R', T') \rightarrow R$ energy-transfer processes. A key process is nonresonant vibrational-to-rotational intramolecular energy transfer in which		

DD FORM 1473  
FACSIMILE

409944

UNCLASSIFIED  
SECURITY CLASSIFICATION OF THIS PAGE (When Data Entered)

72 11 13 084

LB



UNCLASSIFIED

SECURITY CLASSIFICATION OF THIS PAGE(When Data Entered)

19 KEY WORDS (Continued)

20 ABSTRACT (Continued)

HF( $v_1 = 1, J_1$ ) terminates on high  $J_1'$  states of  $v_1' = 0$ . The calculated temperature-dependent quenching rate coefficient for self-relaxation of HF( $v_1 = 1$ ) at temperatures between 300 to 2000 K is dependent on  $v \rightarrow R$  and  $R \rightarrow v$  energy-transfer processes, and beyond 2000 K only on  $v \rightarrow R$  processes. The puzzling temperature dependence observed for HF( $v_1 = 1$ ) vibrational relaxation by HF( $v_2 = 0$ ) is explained by this model. For the high rotational states in the  $v_1' = 0$  manifold, this model predicts incomplete rotational thermalization at low temperatures and complete rotational thermalization at high temperatures. No mechanisms involving dimerization appear to be necessary in understanding the inverse temperature dependence of the reported quenching rate coefficients.

LEVEL II

ACCESSION NO.		
DTIC	White Section <input checked="" type="checkbox"/>	
DDC	Buff Section <input type="checkbox"/>	
UNANNOUNCED	<input type="checkbox"/>	
JUSTIFICATION		
BY		
DISTRIBUTION/AVAILABILITY CODE		
REF.	AVAIL. and/or SPECIAL	
A	.	

DDC  
RECEIVED  
NOV 30 1978  
D

UNCLASSIFIED

SECURITY CLASSIFICATION OF THIS PAGE(When Data Entered)

## PREFACE

The authors gratefully acknowledge Drs. J. F. Bott and J. J. T. Hough for many helpful discussions on several aspects of this study, and Ms. K. L. Foster for her invaluable assistance with the calculations.

CONTENTS

PREFACE . . . . .	1
I. INTRODUCTION . . . . .	7
II. MODEL . . . . .	11
III. RESULTS AND DISCUSSION . . . . .	19
IV. CONCLUSIONS . . . . .	37
REFERENCES . . . . .	39

## FIGURES

1.	Typical computer-generated number-density curves of a laser-induced fluorescence study of HF( $v_1 = 1$ ) + HF( $v_2 = 0$ ) molar concentrations of HF( $v_1 = 1, J = 1$ through 5) versus $t(\mu\text{sec})$ . . . . .	20
2.	Molar concentrations of HF( $v_2 = 0, J_2 = 0$ through 9) versus $t(\mu\text{sec})$ . . . . .	21
3.	Molar concentrations of HF( $v_2 = 0, J_2 = 10$ through 16) versus $t(\mu\text{sec})$ . . . . .	22
4.	Comparison of computer model deduced quenching rate coefficients $k_{\text{emp}}$ with experimental results . . . . .	24
5.	Molar concentration of HF( $v_1' = 0, J_1'$ ) versus rotational quantum number $J_1'$ at various times . . . . .	27
6.	Molar concentrations of HF( $v_1' = 0, J_1'$ ) versus rotational quantum number $J_1'$ at various times . . . . .	28
7.	Molar concentrations of HF( $v_1' = 0, J_1'$ ) versus rotational quantum number $J_1'$ at various times . . . . .	29
8.	Molar concentrations of HF( $v_1' = 0, J_1'$ ) versus rotational quantum number $J_1'$ at various times . . . . .	30
9.	The four terms in Eq. (8) required to calculate $k_{\text{emp}}$ versus $10^3/T$ (K) . . . . .	31
10.	Four terms in Eq. (8) required to calculate $k_{\text{emp}}$ versus $10^3/T$ (K) . . . . .	32

## TABLE

1.	Rate coefficients for $v \rightarrow R$ and $R \rightarrow (R', T')$ energy transfer in HF( $v_1 = 1$ ) + HF( $v_2 = 0$ ) collisions at $T = 300$ K . . . . .	16
----	---	----



## I. INTRODUCTION

The understanding of the temperature dependence generated by the large set of experimental rate coefficients<sup>1-14</sup> for HF( $v_1 = 1$ ) relaxation by HF between 300 and 4000 K hitherto has been incomplete. Bott and Cohen<sup>2</sup> and Hinchey<sup>9</sup> compared these experimental rate coefficients with rate coefficients calculated by means of several theoretical models.<sup>15-18</sup> They concluded that neither the temperature dependence nor the magnitude of the rate coefficient for HF vibrational relaxation is predicted adequately by means of these models.

The experimental rate coefficient for HF( $v = 1$ ) relaxation by HF decreases with increasing temperature from 300 to about 1400 K and increases with increasing temperature beyond 1400 K. This anomalous temperature dependence has been observed in other hydrogen halides and is a basis for speculation that vibrational-to-rotational ( $v \rightarrow R$ ) energy transfer is involved in these interactions. A comparison of isotopic relaxation rates for HCl-HCl and DCl-DCl collisions by Chen and Moore<sup>19</sup> and HBr-HBr and DBr-DBr collisions by Chen and Chen<sup>20</sup> provides convincing evidence that the relaxation of hydrogen halide molecules in the  $v_1 = 1$  vibrational state occurs by a  $v \rightarrow R$  energy-transfer process. Experimental analyses are based on the assumption that the rotational states of HF are equilibrated in about 0.2  $\mu$ sec for a typical pressure of 20 Torr;<sup>8</sup> therefore, rotational equilibrium is assumed in the analyses.<sup>1-10, 12, 13</sup> The possibility of formation of highly excited rotational states of HF by a  $v \rightarrow R$  mechanism in HF( $v_1 = 1$ ) +

HF( $v_2 = 0$ ) collisions and of rotational relaxation from these high rotational states with considerably longer characteristic times has not been considered. This possibility of formation of high rotational states of HF by a  $v \rightarrow R$  mechanism has been suggested, however, by several authors<sup>8, 21, 22</sup> on the basis that the HF( $v_1 = 1$ ) self-relaxation rates observed in pure HF were 30% slower than the similar rates with HF diluted in argon. It was predicted in a previous trajectory study<sup>23</sup> that in HF( $v_1 = 1$ ) + HF( $v_2 = 0$ ) collisions, the vibrationally excited HF rotor removes the energy mismatch  $\Delta E$  that corresponds to rotationless HF molecules by means of a  $v \rightarrow R$  energy-transfer process. This process, which corresponds to nonresonant  $v \rightarrow R$  intramolecular energy transfer, accounts for the formation of highly excited rotational states ( $J'_1 = 10$  through 16) of HF. These high rotational states of HF are slowly relaxed by  $R \rightarrow (T', R')$  energy-transfer processes.

The trajectory study provided temperature-dependent rate coefficients for the formation of HF in high rotational states. These calculated temperature-dependent rate coefficients cannot be compared directly with the experimental temperature-dependent rate coefficient for the vibrational deactivation of HF( $v_1 = 1$ ) in pure HF. The latter should be called an "empirical quenching coefficient" since it represents the net removal rate of HF( $v_1 = 1$ ) through a number of energy transfer channels. The previous analyses used to deduce the experimental results did not consider  $v \rightarrow R$  and  $R \rightarrow v$  energy-transfer processes, which are believed to be important in the vibrational deactivation of HF( $v_1 = 1$ ). In fact, the experimental methods to date are not capable of

measuring directly the actual rate coefficients for the energy-transfer processes predicted by the trajectory study.

The rate coefficients were incorporated for  $v \rightarrow R$ ,  $R \rightarrow v$ ,  $R \rightarrow (T', R')$ , and  $(R', T') \rightarrow R$  energy-transfer processes obtained from the trajectory study into a nonequilibrium kinetic computer program that models the shock tube laser-induced fluorescence technique. This study is designed to determine if this rotational nonequilibrium model can reproduce the experimental temperature-dependent quenching rate coefficients for the vibrational deactivation of  $HF(v_1 = 1)$  by  $HF$ .

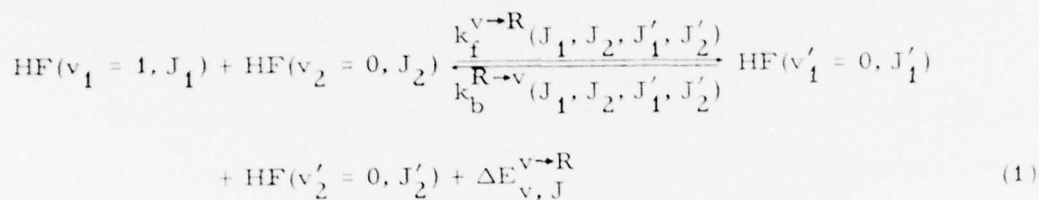
## II. MODEL

A computer code was developed in order to calculate the time-dependent HF( $v_1, J_1$ ) concentrations in defined vibrational  $v_1$  and rotational  $J_1$  states for specific kinetics experiments relevant to energy transfer in HF. This code is an extension of the nonequilibrium chemistry and gasdynamics code<sup>24</sup> (or NEST code) to consider rotational nonequilibrium effects. Until now, in NEST, it was assumed that HF species were in rotational-translational equilibrium at all times, whereas the kinetics between vibrational levels only could be represented. The relation of Wilkins<sup>1,2,3</sup> predicted rate coefficients with experiments can only be understood with a more sophisticated model. As a test of this model, an attempt was made to duplicate the anomalous results of the experimental rate coefficient for HF( $v = 1$ ) self-relaxation, with its pronounced minimum at about 1400 K. Since the principal method of experimental study has been laser-induced fluorescence,<sup>1, 4-10, 12</sup> often coupled with a shock tube<sup>6, 21</sup> or heated cell,<sup>4, 8-10</sup> model initial conditions have been defined to replicate these approaches.

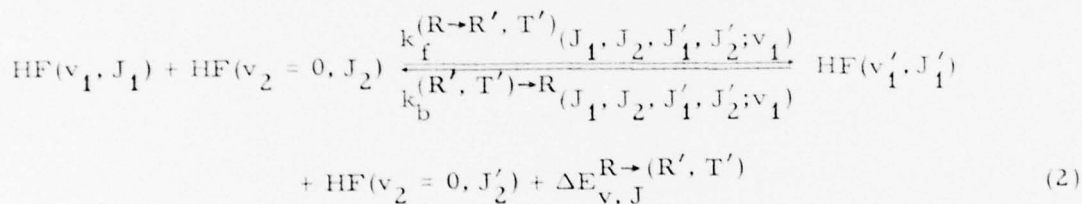
The generation of time-dependent HF( $v_1, J_1$ ) densities by the model is required for comparison with actual experiments. These computer number densities can be summed over  $J_1$ , and the sum then analyzed in the same manner as in actual experiments in order to deduce those empirical quenching coefficients reported by experimentalists. The relationship between these empirical quenching coefficients and rate coefficients for different modes of energy transfer is discussed.



The mechanisms of importance for  $\text{HF}(v_1 = 1, J_1) + \text{HF}$  quenching are described by  $v \rightarrow R$  energy-transfer processes



and rotational-to-rotational-translation energy-transfer process



The  $v \rightarrow R$  processes in Eq. (1) reflect the main results of a recent trajectory study,<sup>23</sup> which predicted that in one out of three  $\text{HF}(v_1 = 1, J_1) + \text{HF}(v_2 = 0, J_2)$  collisions, one quantum of vibrational energy of  $\text{HF}(v_1 = 1, J_1)$  is transferred to rotational energy of the same molecule with almost no change in the distribution of internal energy of the  $\text{HF}(v_2 = 0, J_2)$  molecule. For the range of study  $10 \lesssim J'_1 \lesssim 16$ , the energy defects for the  $v \rightarrow R$  processes in Eq. (1) are much smaller than would be predicted if both reagent and product HF species were assumed to be rotationless. The rotationally excited HF molecules in the  $v'_1 = 0$  vibrational state are relaxed by collisions with other HF molecules by way of the  $\text{R} \rightarrow (\text{R}', \text{T}')$  energy-transfer processes given in Eq. (2).

The  $R \rightarrow (R', T')$  mechanisms with  $\Delta J = -1$  are the main processes for deexcitation of rotationally excited HF species. The  $\text{HF}(v_1' = 0, J_1')$  species at low temperatures will have a nonequilibrium distribution of the high rotational states because, at high values of  $J$ , spacing between the rotational levels is so large that a few collisions will not cause rotational relaxation by  $\Delta J = -1$  transitions. In trajectory study,<sup>23</sup> it was predicted that rotational relaxation from the high  $J$  levels to the low  $J$  levels with multiple quantum  $J$ -transitions is a very inefficient process. A transition from  $J = 3$  to  $J = 2$  occurs about one in three collisions, whereas a multiquantum transition from  $J = 15$  to  $J = 12$  occurs about 1 in 1000 collisions, or a transition from  $J = 3$  to  $J = 0$  occurs about 1 in 50 collisions. Even at low  $J$  levels, the probability of multiquantum transitions are at least one order of magnitude smaller than the probability of a single-quantum transition. In this study, only single-quantum deactivation processes are used for the  $R \rightarrow (R', T')$  mechanisms for relaxing the rotationally excited states of HF.

The generalized rate equations for the  $v \rightarrow R$  and  $R \rightarrow (T', R')$  energy transfer processes in Eqs. (1) and (2) are given as

$$\frac{d[\text{HF}(v_1 = 1, J_1)]}{dt} = - \sum_{J_2} \sum_{J_2'} \sum_{J_1'=10}^{16} k_f^{v \rightarrow R}(J_1, J_2, J_1', J_2') [\text{HF}(v_1 = 1, J_1)] \times [\text{HF}(v_2 = 0, J_2)]$$

(cont.)

$$\begin{aligned}
& + \sum_{J_2} \sum_{J_2'} \sum_{J_1'=10}^{16} k_b^{R \rightarrow v}(J_1, J_2, J_1', J_2') [\text{HF}(v_1' = 0, J_1')] \\
& \quad \times [\text{HF}(v_2' = 0, J_2')] \\
& - \sum_{J_2} \sum_{J_2'} \sum_{J_1'} k_f^{R \rightarrow (R', T')}(J_1, J_2, J_1', J_2'; v_1 = 1) \\
& \quad \times [\text{HF}(v_1 = 1, J_1)] [\text{HF}(v_2 = 0, J_2)] \\
& + \sum_{J_2} \sum_{J_2'} \sum_{J_1'} k_b^{(T', R') \rightarrow R}(J_1, J_2, J_1', J_2'; v_1 = 1) \\
& \quad \times [\text{HF}(v_1' = 1, J_1')] [\text{HF}(v_2' = 0, J_2')] \quad (3)
\end{aligned}$$

$$\begin{aligned}
\frac{d[\text{HF}(v_1' = 0, J_1' \geq 10)]}{dt} & = \sum_{J_1} \sum_{J_2} \sum_{J_2'} k_f^{v \rightarrow R}(J_1, J_2, J_1', J_2') [\text{HF}(v_1 = 1, J_1)] \\
& \quad \times [\text{HF}(v_2 = 0, J_2)] \\
& - \sum_{J_1} \sum_{J_2} \sum_{J_2'} k_b^{R \rightarrow v}(J_1, J_2, J_1', J_2') [\text{HF}(v_1' = 0, J_1')] \\
& \quad \times [\text{HF}(v_2' = 0, J_2')] \\
& - \sum_{J_1''} \sum_{J_2} \sum_{J_2'} k_f^{R \rightarrow (R', T')}(J_1, J_2, J_1'', J_2'; v_1 = 0) \\
& \quad \times [\text{HF}(v_1' = 0, J_1')] [\text{HF}(v_2 = 0, J_2')]
\end{aligned}$$

(cont.)

$$\begin{aligned}
& + \sum_{J_1''} \sum_{J_2} \sum_{J_2'} k_b^{(R', T') \rightarrow R} (J_1', J_2, J_1'', J_2'; v_1 = 0) \\
& \times [\text{HF}(v_1' = 0, J_1'')] [\text{HF}(v_2' = 0, J_2')] \quad (4)
\end{aligned}$$

and

$$\begin{aligned}
\frac{d[\text{HF}(v_1' = 0, J_1' < 10)]}{dt} = & - \sum_{J_1'} \sum_{J_2} \sum_{J_2'} k_f^{R \rightarrow (R', T')} (J_1', J_2, J_1', J_2'; v_1 = 0) \\
& \times [\text{HF}(v_1 = 0, J_1)] [\text{HF}(v_2 = 0, J_2)] \\
& + \sum_{J_1'} \sum_{J_2} \sum_{J_2'} k_b^{(R', T') \rightarrow R} (J_1', J_2, J_1', J_2'; v_1 = 0) \\
& \times [\text{HF}(v_1' = 0, J_1')] [\text{HF}(v_2' = 0, J_2')] \quad (5)
\end{aligned}$$

Equations (3), (4), and (5) provide a coupled set of first-order differential equations solvable by the use of NEST.<sup>24</sup> The rate coefficients  $k_f^{v \rightarrow R}$  and  $k_f^{R \rightarrow (T', R')}$  depend on the eight quantum numbers ( $v_1, J_1, v_2, J_2, v_1', J_1', v_2', J_2'$ ). In Table 1 are given the  $k_f^{v \rightarrow R}$  and  $k_f^{R \rightarrow (T', R')}$  rate coefficients used to calculate the quenching rate coefficient for self-relaxation of  $\text{HF}(v_1 = 1)$  at 300 K.

The initial conditions for the computation simulate a laser-induced fluorescence experiment. At a given temperature, pressures of  $[\text{HF}(v_2 = 0)] = \sum_{J_2} [\text{HF}(v_2 = 0, J_2)]$  up to 0.5 Torr were used. The initial amount of rotationally equilibrated  $\text{HF}(v_1 = 1) = \sum_{J_1} [\text{HF}(v_1 = 1, J_1)]$  is taken to be 0.01 of  $[\text{HF}(v_2 = 0)]$ .



Table 1. Rate coefficients<sup>a</sup> for  $v \rightarrow R$  and  $R \rightarrow (R', T')$  energy transfer in  $\text{HF}(v_1 = 1) + \text{HF}(v_2 = 0)$  collisions at  $T = 300 \text{ K}$

$v \rightarrow R$ Rates	$10^{-11} k_f^{v \rightarrow R}$ , $\text{cm}^3/\text{mol-sec}$
$\text{HF}(1, 0) + \text{HF}(0, J_2) \rightarrow \text{HF}(0, J'_1) + \text{HF}(0, J_2)$	1.3
$\text{HF}(1, 1) + \text{HF}(0, J_2) \rightarrow \text{HF}(0, J'_1) + \text{HF}(0, J_2)$	6.4
$\text{HF}(1, 2) + \text{HF}(0, J_2) \rightarrow \text{HF}(0, J'_1) + \text{HF}(0, J_2)$	13.0
$\text{HF}(1, 3) + \text{HF}(0, J_2) \rightarrow \text{HF}(0, J'_1) + \text{HF}(0, J_2)$	9.1
$\text{HF}(1, 4) + \text{HF}(0, J_2) \rightarrow \text{HF}(0, J'_1) + \text{HF}(0, J_2)$	5.1
$\text{HF}(1, 5) + \text{HF}(0, J_2) \rightarrow \text{HF}(0, J'_1) + \text{HF}(0, J_2)$	5.1
$R \rightarrow (R', T')$ Rates	$10^{-11} k_f^{R \rightarrow (R', T')}$ , $\text{cm}^3/\text{mol-sec}$
$\text{HF}(0, 16) + \text{M} \rightleftharpoons \text{HF}(0, 15) + \text{M}$	3.3
$\text{HF}(0, J'_1) + \text{M} \rightleftharpoons \text{HF}(0, J'_1 - 1) + \text{M}$ , $J'_1 = 15, \dots, 11$	6.6
$\text{HF}(0, J'_1) + \text{M} \rightleftharpoons \text{HF}(0, J'_1 - 1) + \text{M}$ , $J'_1 = 10, \dots, 6$	11.
$\text{HF}(0, J'_1) + \text{M} \rightleftharpoons \text{HF}(0, J'_1 - 1) + \text{M}$ , $J'_1 = 5, \dots, 1$	21.

<sup>a</sup> $J'_1 = 16, 15, \dots, 10, J_2 = 0, 1, \dots, 5$ . To obtain rate coefficient for  $v \rightarrow R$  relaxation of  $\text{HF}(v_1 = 1, J_1)$  by  $\text{HF}(v_2 = 0, J_2)$ , multiply  $k_f^{v \rightarrow R}$  by  $(2J_2 + 1) \cdot \exp[-E(v_2 = 0, J_2)/kT]/Q_R(v_2, J_2)$ , where  $Q_R(v_2, J_2)$  is the total rotational partition function.

at temperatures from 300 to 1000 K, 0.1 from 1000 to 1500 K and 0.2 from 1600 to 2400 K. Since the  $[\text{HF}(v_1 = 1)]$  concentration is generally much less than that for  $[\text{HF}(v_1 = 0)]$ , in Eq. (3)  $v \rightarrow v$  pumping processes that involve collisions of two  $\text{HF}(v_1 = 1)$  molecules have been neglected.

The Landau-Teller theory<sup>25</sup> for an harmonic oscillator gives the relationship for the time rate of change of number density  $n_1(t)$  at the instantaneous translational temperature

$$\frac{1}{\tau} = \frac{1}{[n_1(t) - n_1(t = \infty)]} \left( - \frac{dn_1}{dt} \right) \quad (6)$$

where  $n_1(t = \infty)$  is the equilibrium number density of the  $v = 1$  vibrational state and  $\tau$  is the relaxation time of the bimolecular collisional deactivation mechanism. The empirical quenching rate coefficient  $k_{\text{emp}}$  obtained from Eq. (6) can be written as

$$k_{\text{emp}} = \frac{1}{[\text{HF}(v = 0)]} \cdot \frac{1}{\{[\text{HF}(v = 1)] - [\text{HF}(v = 1)]_{\text{eq}}\}} \cdot \left( - \frac{d[\text{HF}(v = 1)]}{dt} \right) \quad (7)$$

From Eq. (3) with application of Eq. (7), the empirical quenching rate coefficients depend on the  $v \rightarrow R$  and  $R \rightarrow v$  energy-transfer processes.

### III. RESULTS AND DISCUSSION

Typical results from the calculation are shown in Figs. 1 through 3. The logarithmic densities of HF( $v = 1, J$ ) and HF( $v = 0, J$ ) are plotted as a function of time. An essentially exponential decay is computed for HF( $v_1 = 1, J_1$ ). As with the actual experiments, the empirical quenching coefficient  $k_{emp}$  is deduced through Eq. (7). The calculation is performed at several HF densities in order to verify that  $k_{emp}$  is indeed the result of HF quenching. The slope of the inverse characteristic decay times versus HF( $v = 0$ ) densities yields the same computed value of  $k_{emp}$ . This procedure has been used by experimentalists to ensure that the deduced observed quenching coefficient is not effected by competing or secondary processes. Thus, the analytical techniques of the experimental workers have been duplicated exactly.

Vibrational-to-rotational processes predominately cause the high  $J$  states of HF( $v = 0, J$ ), corresponding to the  $J_1'$  states of Eq. (1), to depart significantly from equilibrium in Figs. 2 and 3. For example, at  $t = 50 \mu\text{sec}$ , HF( $v = 0, J = 13$ ) is four orders of magnitude greater than its equilibrium density. In this model, rotational inversions are also computed for some  $J$  in limited time domains.

In Figs. 1 through 3, the initial amount of rotational equilibrated HF( $v_1 = 1$ ) is taken to be 0.01 of HF( $v_2 = 0$ ). For this case, the densities of the HF( $v_1' = 0, J_1' = 10, \dots, 14$ ) after 50  $\mu\text{sec}$  are equivalent to those of the initial

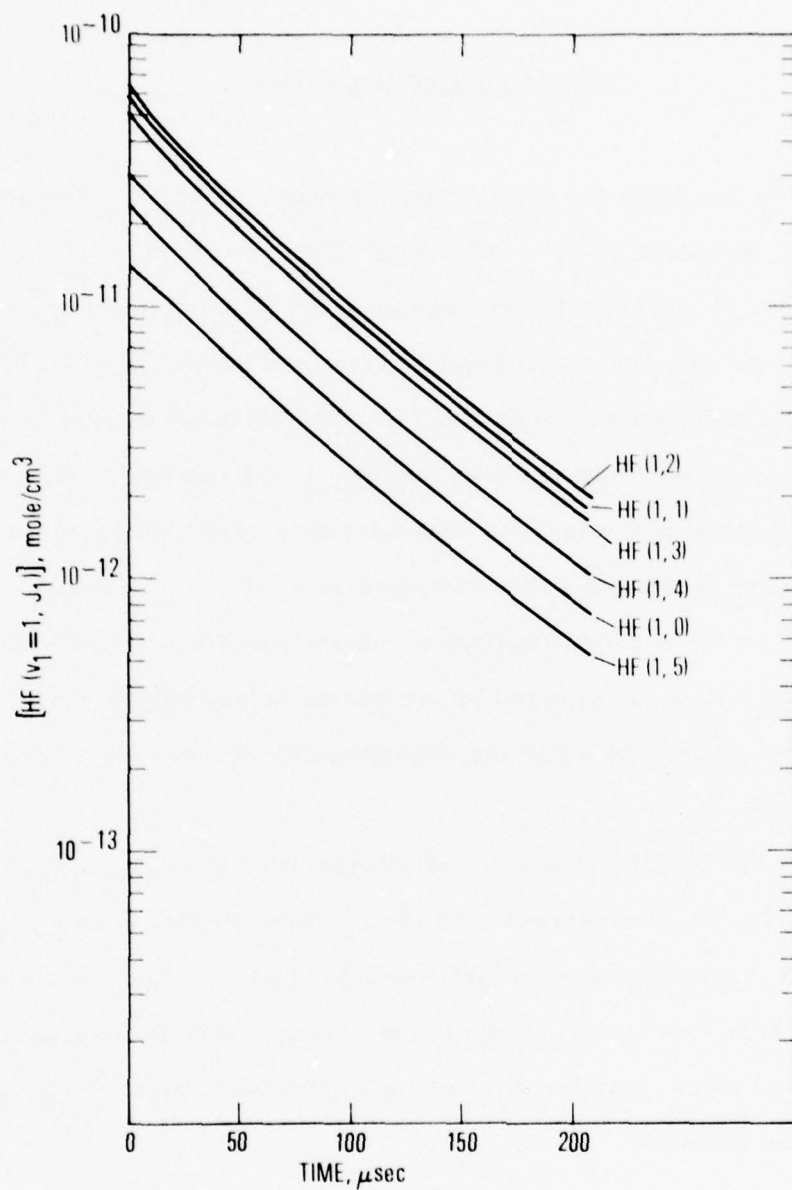


Fig. 1. Typical computer-generated number-density curves of a laser-induced fluorescence study of HF( $v_1 = 1$ ) + HF( $v_2 = 0$ ) molar concentrations of HF( $v_1 = 1$ ,  $J = 1$  through 5) versus  $t$ ( $\mu\text{sec}$ ).  $T = 300$  K,  $P = 0.47$  Torr.



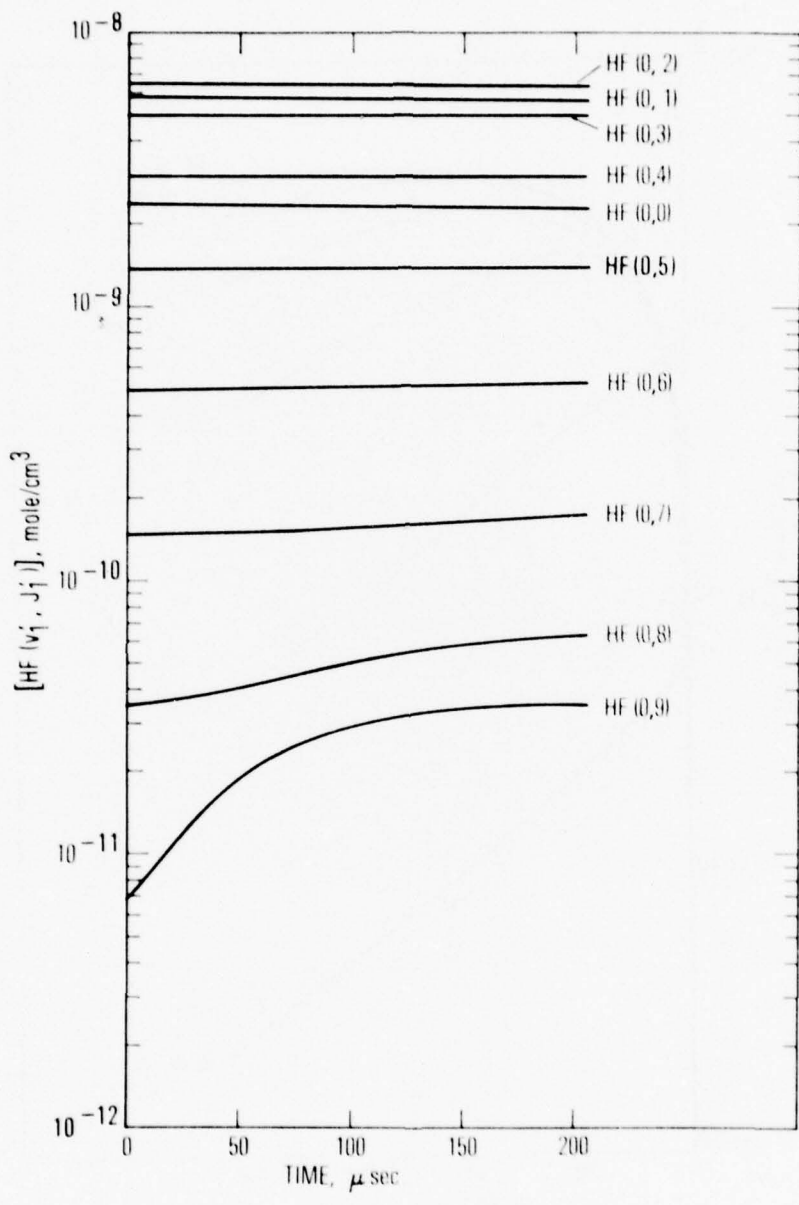


Fig. 2. Molar concentrations of HF( $v_2 = 0, J_2 = 0$  through 9) versus  $t(\mu\text{sec})$ .  $T = 300$  K,  $P = 0.47$  Torr.

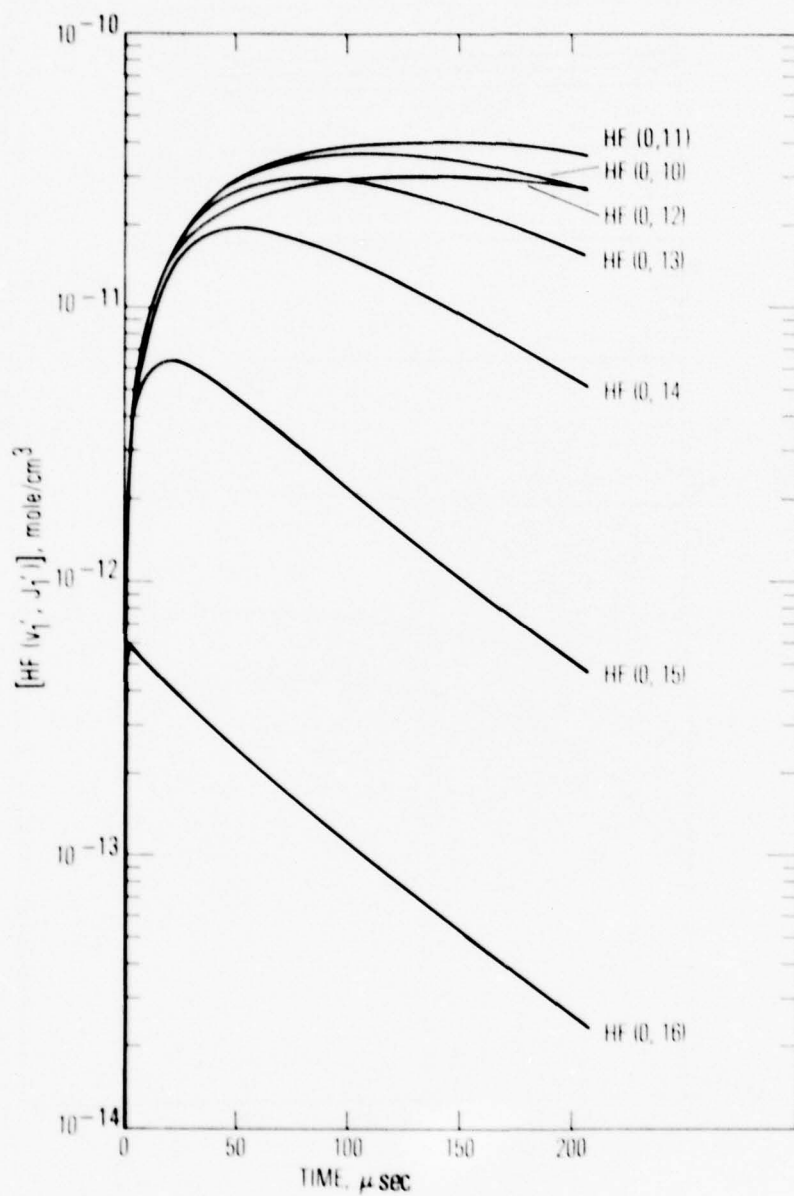


Fig. 3. Molar concentrations of HF( $v_2 = 0, J_2 = 10$  through 16) versus  $t(\mu\text{sec})$ .  $T = 300 \text{ K}$ ,  $P = 0.47 \text{ Torr}$ .

HF( $v_1 = 1, J_1$ ) states. If only 0.1% of the HF( $v_2 = 0$ ) molecules are pumped into HF( $v_1 = 1$ ) state, similar calculations indicate that the densities of the HF( $v_1' = 0, J_1' = 10, \dots, 14$ ) after 50  $\mu$ sec are down by almost an order of magnitude from those of the 1.0% pumped case. These computed results mean that the presence of the  $J_1'$  states would be difficult to detect and that the magnitude of these  $J_1'$  state densities are quite sensitive to initially excited vibrational-rotational states.

The inverse of the quenching rate coefficient is shown on a traditional Landau-Teller plot in Fig. 4, where  $P\tau$  is plotted as a function of  $T^{-1/3}$ . The calculated quenching coefficient  $P\tau$ , depicted for pedagogical purposes by large open circles, is in quite good agreement with the available experimental data. It increases with increasing temperature up to 1371 K, levels off at about 1400 K, and then begins to decrease. The range of study is 300 to 2400 K. Thus, the model is able to replicate the behavior of the empirical quenching coefficient for HF( $v = 1$ ) + HF relaxation.

The agreement of  $k_{\text{emp}}$  is within 5% of Bott<sup>6</sup> and Osgood<sup>7</sup> results at 300 K but 34% smaller than that of Stephen.<sup>4</sup> At 1000 K, the agreement with Bott<sup>6</sup> and Hitchen<sup>9</sup> is excellent, whereas  $k_{\text{emp}}$  is 30% smaller than the quenching coefficient of Blair.<sup>12</sup> At 2400 K, agreement within 10% of the results of Bott,<sup>2</sup> Vasil'ev,<sup>11</sup> and Just<sup>13</sup> is still achieved; but this computed  $k_{\text{emp}}$  is 43% smaller than the number of Solomon<sup>3</sup> or Blair.<sup>12</sup> When it is considered that our model is constructed from theoretical cross sections (Table 1) without adjustment of parameters, the general agreement over the entire temperature range with experiments is quite satisfactory.

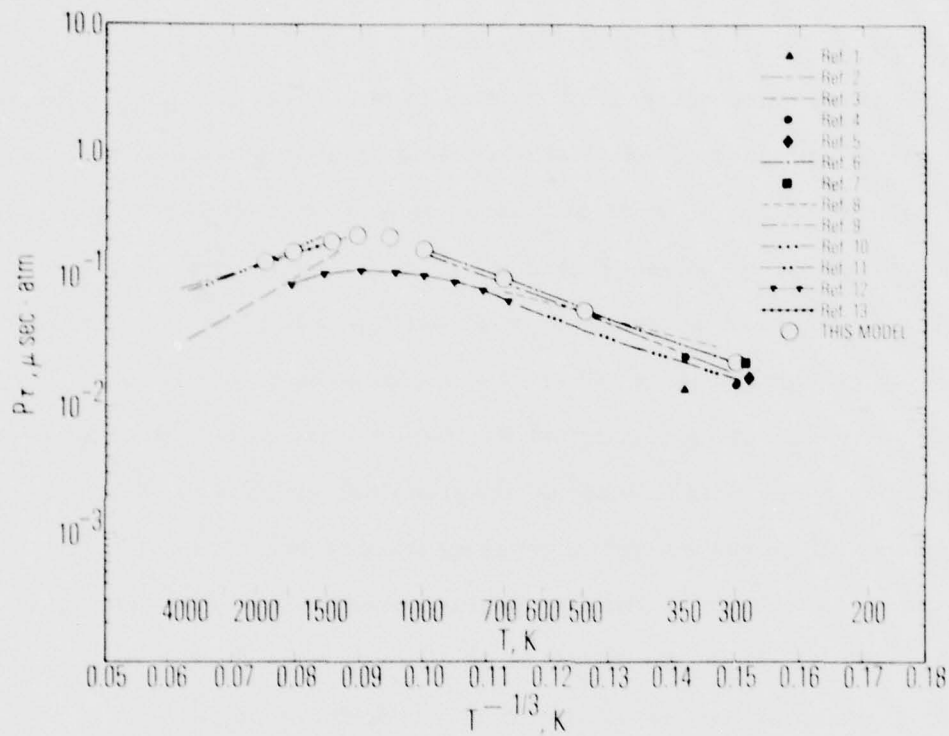


Fig. 4. Comparison of computer model deduced quenching rate coefficients  $k_{\text{emp}}$  with experimental results. Vibrational relaxation times for deactivation HF( $v = 1$ ) by HF.  $P_T$  values are plotted versus  $T^{-1/3}$ .

This model provides a satisfactory description of HF relaxation without invoking the formation of collision complexes. The formation of HF dimers has been proposed by several authors<sup>1, 26, 29</sup> in order to explain the temperature dependence in vibrational relaxation of HF( $v_1 = 1$ ) by HF. Trajectory calculations by Wilkins<sup>23</sup> indicate that collision complexes are not formed in HF + HF collisions in the temperature range at or above 300 K. The trajectory calculations indicate that the HF( $v_1 = 1$ ) + HF( $v_2 = 0$ ) collisions, the vibrational energy of the vibrationally excited HF molecule is transferred into rotational energy of the same molecule. The energy defects are much smaller in these  $v \rightarrow R$  processes than what would have been predicted if both reagent and product HF species were assumed to be rotationless. The long-range attractive forces in HF-HF collisions reduce the steepness of the short-range repulsive forces in HF-HF collisions and thereby permit more conversion of vibrational energy. The near-resonant  $v \rightarrow R$  transitions are not important in explaining HF( $v_1 = 1$ ) vibrational relaxation in pure HF.

The experimental or empirical quenching coefficient  $k_{\text{emp}}$  represents not one unique rate coefficient but a complex sum of a number of rate terms for several energy transfer channels available. Regions of temperature in Fig. 4 can now be delineated as to which particular processes contribute to  $k_{\text{emp}}$ ; these are discussed later in this work.

The calculated time-dependent HF( $v = 0, J$ ) concentrations at temperatures of 300, 500, 700, and 1000 K are presented as a function of the rotational



quantum number  $J'$  in Figs. 5 through 8. At low temperatures, the low rotational states ( $J' < 8$ ) have a Boltzmann distribution; the high rotational states ( $J' > 8$ ) exhibit a non-Boltzmann distribution. At high temperatures ( $T > 700$  K), all of the rotational states exhibit a Boltzmann distribution. In Fig. 5 is shown the incomplete thermalization of the high rotational  $J$ -levels during vibrational relaxation of  $\text{HF}(v_1 = 1)$  in pure HF. The maximum rotational nonequilibrium in the high rotational states at about  $t = 50 \mu\text{sec}$ . As  $t$  increases from 50 to 800  $\mu\text{sec}$ , the high rotational states tend to relax rotationally toward the Boltzmann distribution indicated at  $t = 0 \mu\text{sec}$ . In Fig. 5, inverted behavior of some of the high  $J$  or  $J'_1$  states with time can be observed.

From Eq. (7),  $k_{\text{emp}}$  can be written as

$$k_{\text{emp}} = \frac{1}{[\text{HF}(v_2 = 0)]} \frac{1}{\{[\text{HF}(v_1 = 1)] - [\text{HF}(v_1 = 1)]_{\text{eq}}\}} (L_f - L_b) \quad (8)$$

The  $L_f$  and  $L_b$  terms represent the total rate contributions to  $(-dn_1/dt)$  from  $v \rightarrow R$  and  $R \rightarrow v$  processes, respectively. In Fig. 9, are curves representing the temperature dependency of the four parts of the expression for  $k_{\text{emp}}$ :  $L_f$ ,  $L_b$ ,  $[\text{HF}(v_2 = 0)]^{-1}$ , and  $\{[\text{HF}(v_1 = 1)] - [\text{HF}(v_1 = 1)]_{\text{eq}}\}^{-1}$ . The initial amount of  $\text{HF}(v_1 = 1)$  is 0.01 that of  $\text{HF}(v_2 = 0)$ . In Fig. 10, another four curves are exhibited for the high-temperature conditions; initial  $\text{HF}(v_1 = 1)$  is 0.1 of initial  $\text{HF}(v_2 = 0)$ . From the curves given in Figs. 9 and 10, both  $v \rightarrow R$  and  $R \rightarrow v$  processes are important from 300 to 2000 K

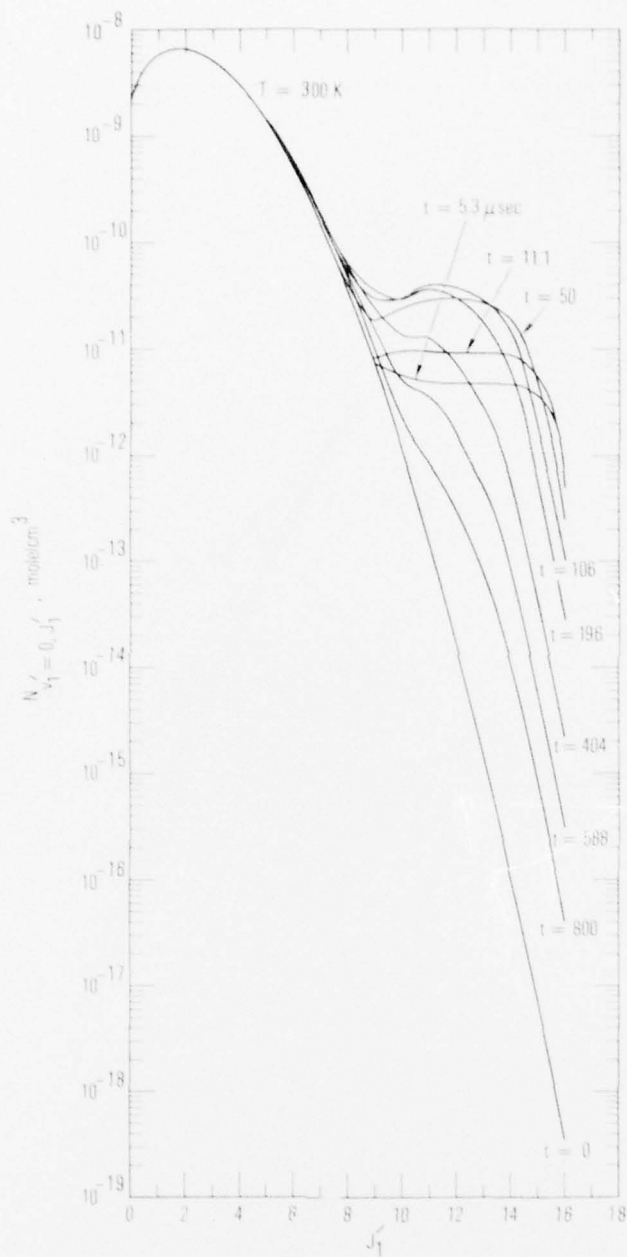


Fig. 5. Molar concentration of HF( $v_1' = 0, J_1'$ ) versus rotational quantum number  $J_1'$  at various times.  $T = 300$  K,  $P = 0.47$  Torr.

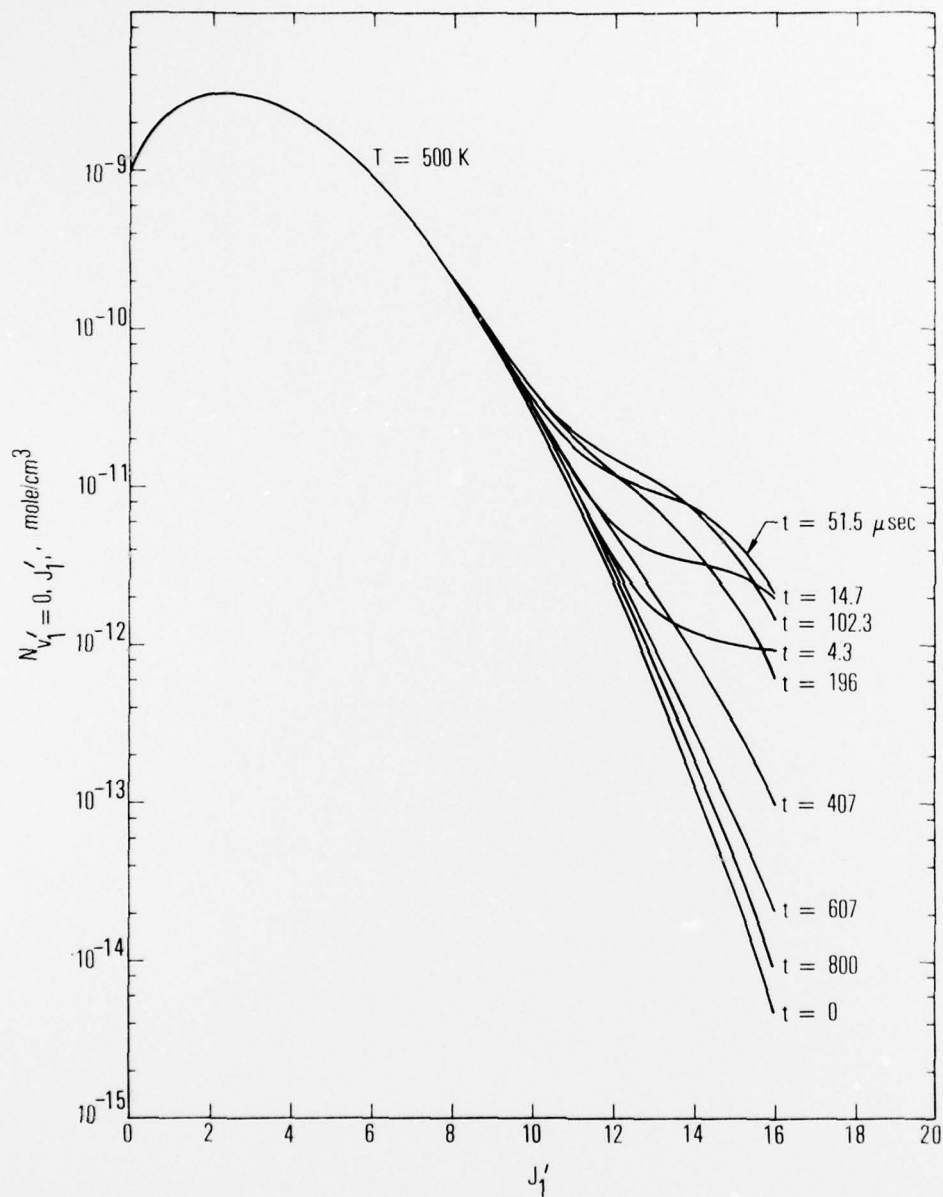


Fig. 6. Molar concentrations of HF( $v'_1 = 0, J'_1$ ) versus rotational quantum number  $J'_1$  at various times.  $T = 500$  K,  $P = 0.47$  Torr.

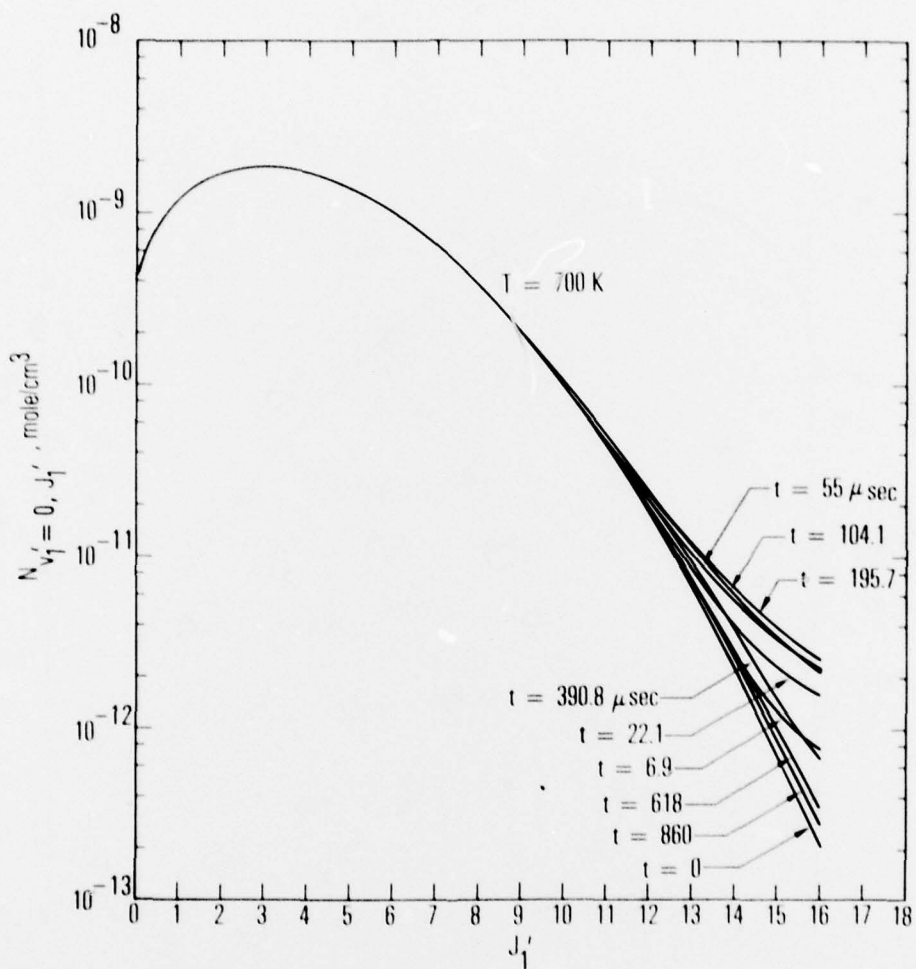


Fig. 7. Molar concentrations of HF( $v'_1 = 0, J'_1$ ) versus rotational quantum number  $J'_1$  at various times.  $T = 700$  K,  $P = 0.47$  Torr.

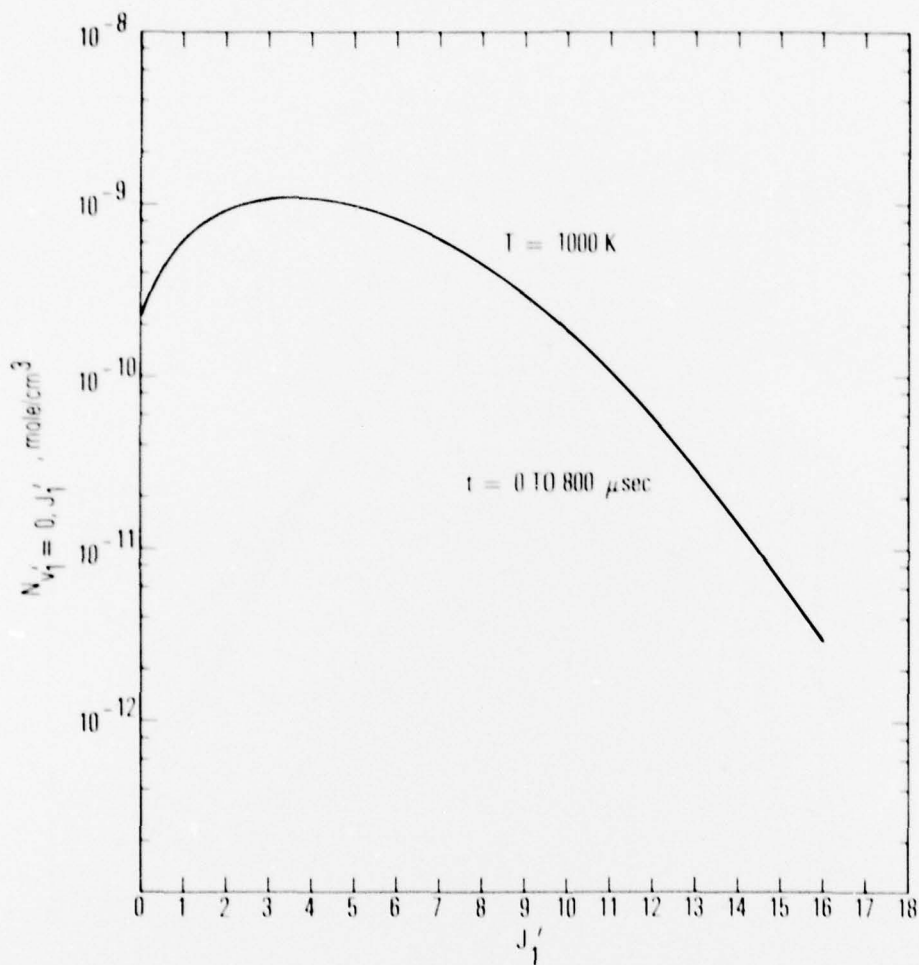


Fig. 8. Molar concentrations of HF( $v'_1 = 0, J'_1$ ) versus rotational quantum number  $J'_1$  at various times.  $T = 1000 \text{ K}$ ,  $P = 0.47 \text{ Torr}$ .



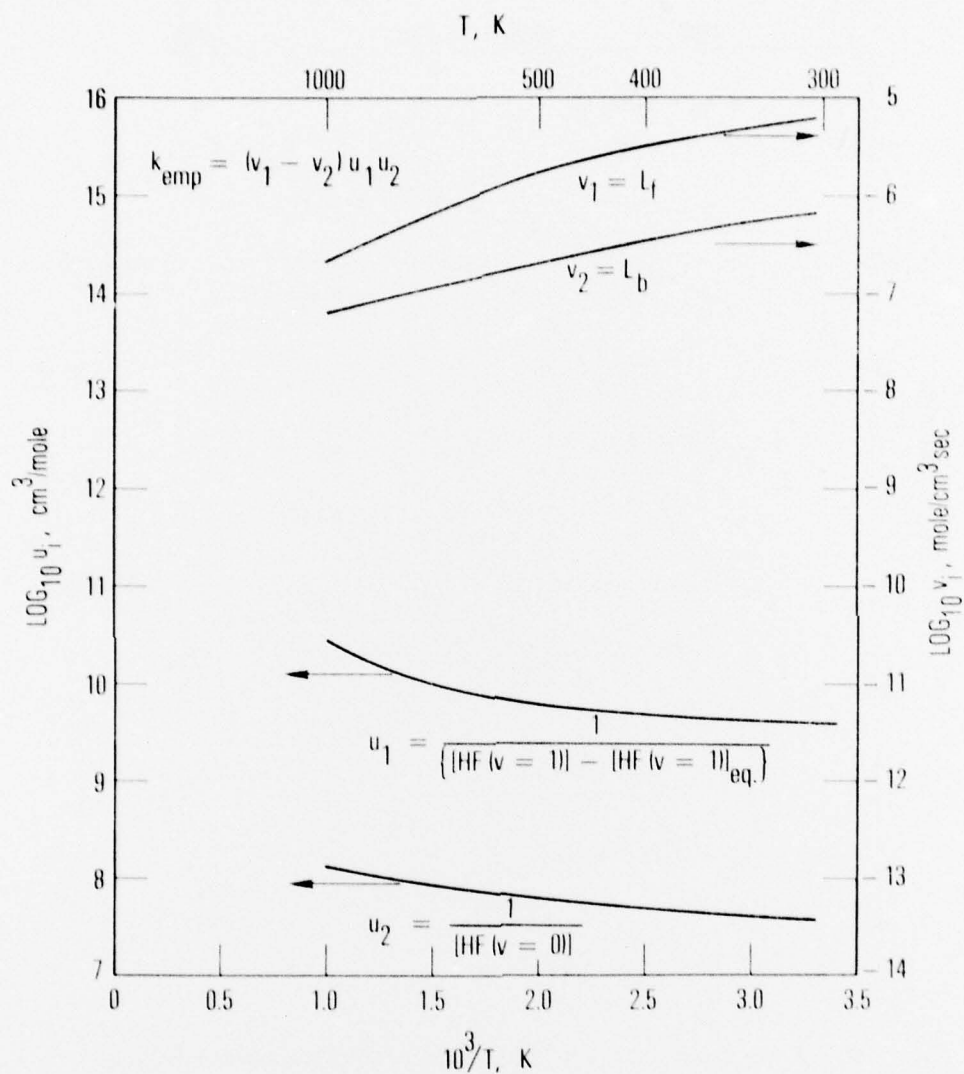


Fig. 9. The four terms in Eq. (8) required to calculate  $k_{emp}$  versus  $10^3/T$  (K).  $HF(v_1 = 1)$  was taken to be 0.01 of  $HF(v_2 = 0)$ .  $L_f$  is the rate of  $v \rightarrow R$  processes affecting  $d[HF(v = 1)]/dt$ .  $L_b$  is the rate of  $R \rightarrow v$  processes.  $t = 10 \mu\text{sec}$ ,  $P = 0.47$  Torr.

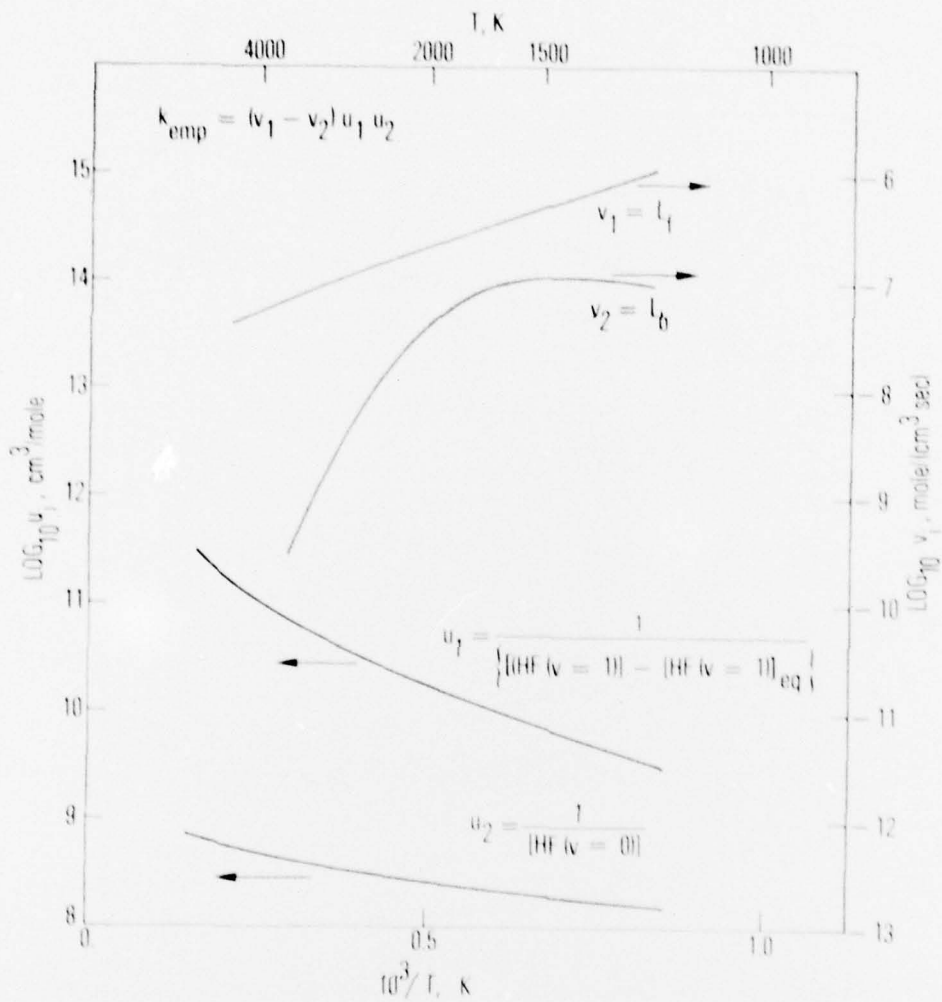


Fig. 10. Four terms in Eq. (8) required to calculate  $k_{\text{emp}}$  versus  $10^3/T$  (K).  $\text{HF}(v_1 = 1)$  was taken to be 0.1 of  $\text{HF}(v_2 = 0)$ ,  $t = 10 \mu\text{sec}$ ,  $P = 0.47 \text{ Torr}$ .

and beyond 2000 K, only the  $v \rightarrow R$  processes are important. The contributions from  $v \rightarrow R$  processes decrease monotonically with increasing temperature. The contributions from  $R \rightarrow v$  processes decrease with increasing temperature. The expression  $L_f - L_b$ , therefore, exhibits a decreasing slope with increasing temperature or a concave-up behavior for  $k_{emp}$ . The ascending high-temperature leg of  $k_{emp}$  (or descending leg of  $P$ ) depends very much on the Landau-Teller analytical interpretation used by experimentalists<sup>2, 12</sup> and the fact that  $\{[HF(v = 1)] = [HF(v = 1)]_{eq}\}$  becomes much smaller at higher temperatures, which gives the "normal" appearance of a rate coefficient with a  $T^{-1/3}$  dependence. Without this interpretation and division by the difference of two densities, the high-temperature leg of  $k_{emp}$  cannot be reproduced by the model. The model also indicates that even though a Boltzmann distribution of  $J$  states is maintained at all times above 1000 K (Fig. 8), the functional behavior of  $L_f$ ,  $L_b$ , and  $\{[HF(v = 1)] - [HF(v = 1)]_{eq}\}$  generates the minimum and increasing leg of  $k_{emp}$ .

It appears that  $k_{emp}$  is a net summation of a series of rate terms representing available channels for  $v \rightarrow R$  and  $R \rightarrow v$  mechanisms. Each rate term is essentially a collision frequency consisting of a product of rate coefficients and densities of colliding molecules, Eqs. (3), (4), and (5). In general,  $k_{emp}$  can have significantly larger or smaller values than the individual  $k_f^{v \rightarrow R}(J_1, J_2, J'_1, J'_2)$  terms. Moreover, the temperature dependence of  $k_{emp}$  need not have the same behavior as the individual  $k_f^{v \rightarrow R}(J_1, J_2, J'_1, J'_2)$  terms. It follows then that the rotationless energy defect, definable from experiments on  $k_{emp}$  as  $3961 \text{ cm}^{-1}$ , also has no meaning when determining a

"backward" quenching rate coefficient. The individual energy defects  $\Delta E_{v,J}$ , as defined by Eq. (1), are much smaller.

Evidence of high  $J'_1$  states in significant rotational nonequilibrium conditions is crucial evidence in establishing validity for the  $v \rightarrow R$  processes and this model. The densities in Fig. 3 indicate some rotational population inversions, which means that laser action on pure rotational transitions of HF might be possible. For example, Deutsch<sup>30</sup> observed laser action on pure rotational transitions of HF formed by the  $F + H_2$  chemical reaction. He observed rotational transitions in HF from energy levels corresponding to very high  $J$  values, which indicates a rotational nonequilibrium distribution of  $HF(v, J_{\text{high}})$  states. The rotational states responsible for the laser action observed by Deutsch could not have been formed from the  $F + H_2$  reactions.<sup>23</sup> It would appear that the high  $J$  states observed may have been formed by energy-transfer processes involving vibrational relaxation from high  $(v, J)$  levels of HF where multi-quantum  $v \rightarrow R$  energy-transfer processes are important. This is believed to provide a plausible explanation for the high  $J$ -states observed by Deutsch. Krough<sup>31</sup> has reported lasing in flash-photolysis-initiated HF chemical lasers involving exceptionally high  $J$  states and has invoked versions of the  $v \rightarrow R$  mechanism to explain the results.

Some indication of rotational nonequilibrium has been given by Green, Sanders, and Hancock,<sup>21, 22, 32</sup> who measured  $HF(v = 1)$  self-relaxation rates in pure HF in HF highly diluted with argon by means of the laser-excited vibrational fluorescence technique. They found that  $HF(v_1 = 1)$  self-relaxation rate observed in pure HF was 30% slower than the similar rate with HF diluted

in argon. They speculated that this behavior was a result of incomplete thermalization of the high rotational states during vibrational relaxation in pure HF. If it is assumed that a quantum of vibrational energy of the HF( $v_1 = 1$ ) molecule goes mostly into rotational energy of the same molecule upon an HF( $v_1 = 1$ ) + HF( $v_2 = 0$ ) collision, the  $v \rightarrow R$  mechanism would give a large  $\Delta J$  change with a very small energy defect. In Fig. 5, the incomplete thermalization of the rotational levels speculated on by Green, Sanders, and Hancock is shown. Such evidence is considered to be indirect, however, and an unambiguous experiment, which reveals very high J states out of equilibrium as a result of the  $v \rightarrow R$  processes in HF, is still to be performed.



#### IV. CONCLUSIONS

The empirical quenching coefficient for  $\text{HF}(v_1 = 1) + \text{HF}$  vibrational relaxation has been successfully duplicated with good agreement over the entire temperature range with the use of a rotational nonequilibrium model and rate coefficients computed by Wilkins.<sup>23</sup> The key processes are  $v \rightarrow R$  and  $R \rightarrow v$  mechanisms, which give the problem a multiple-channel nature. The puzzling temperature dependence<sup>33</sup> observed for  $\text{HF}(v_1 = 1)$  vibrational relaxation by  $\text{HF}(v_2 = 0)$  is explained by this model. This model should be equally applicable to vibrational relaxation of other hydrogen halide molecules. This theoretical study is the first in which  $\text{HF}(v_1 = 1)$  vibrational relaxation by  $\text{HF}(v_2 = 0)$  has been fully described over the entire temperature range. It also confirms previous high ( $>1400$  K) and low ( $<1000$  K) temperature experimental studies. No mechanisms involving dimerization appear to be necessary to an understanding of the inverse temperature dependence of the reported quenching rate coefficients.

Significant high rotational state nonequilibria are predicted by Wilkins and this kinetic model at the low temperatures. An attempt by us to experimentally observe these high J states is in progress.

## REFERENCES

1. J. R. Airey and S. S. Fried, Chem. Phys. Lett. **8**, 23 (1971).
2. J. F. Bott and N. Cohen, J. Chem Phys. **55**, 3698 (1971).
3. W. C. Solomon, J. A. Blauer, F. C. Jaye, and J. G. Hnat, Int. J. Chem. Kinetics **3**, 215 (1971).
4. R. R. Stephen and T. A. Cool, J. Chem. Phys. **56**, 5863 (1972).
5. J. K. Hancock and W. H. Green, J. Chem. Phys. **57**, 4515 (1972).
6. J. F. Bott, J. Chem. Phys. **57**, 96 (1972).
7. R. M. Osgood, Jr., A. Javan, and P. B. Sackett, Appl. Phys. Lett. **20**, 269 (1972); J. Chem. Phys. **60**, 1464 (1973).
8. S. S. Fried, J. Wilson, and R. L. Taylor, IEEE J. Quantum Electron. **QE-9**, 59 (1973).
9. J. J. Hinchey, J. Chem. Phys. **59**, 223, 2224 (1973).
10. R. A. Lucht and T. A. Cool, J. Chem. Phys. **60**, 1026 (1974).
11. G. K. Vasil'ev, E. F. Makarov, V. G. Papin, and V. L. Tal'roze, Zh. Eksp. Teor. Fiz **64**, 2046 (1973).
12. L. S. Blair, W. D. Breshears, and G. L. Schott, J. Chem. Phys. **59**, 1582 (1973).
13. T. Just and G. Rimpel, "Studies of HF Relaxation and on the Reaction of  $H_2$  with  $F_2$  Behind Shocks," presented at 3rd Conference on Chemical and Molecular Lasers, St. Louis, Missouri, May 1972.
14. M. A. Kwok and R. L. Wilkins, J. Chem. Phys. **63**, 2453 (1975).

15. R. N. Schwartz, A. I. Slawsky, and K. F. Herzfeld, J. Chem. Phys. 20, 1591 (1952).
16. H. K. Shin, Chem. Phys. Lett. 6, 494 (1970); J. Phys. Chem. 75, 1079 (1971).
17. C. B. Moore, J. Chem. Phys. 43, 2979 (1965).
18. G. C. Berend and R. L. Thommarson, J. Chem. Phys. 58, 3203 (1973).
19. H. L. Chen and C. B. Moore, J. Chem. Phys. 54, 4072 (1971).
20. M. Y. D. Chen and H. L. Chen, J. Chem. Phys. 56, 3315 (1972).
21. W. H. Green and J. K. Hancock, IEEE J. Quantum Electron. QE-9, 50 (1973).
22. J. K. Hancock and W. H. Green, J. Chem. Phys. 57, 4515 (1972).
23. R. L. Wilkins, J. Chem. Phys. 67, 5838 (1977).
24. E. B. Turner, G. Emanuel, and R. L. Wilkins, The NEST Chemistry Computer Program, TR-0059(6240-40)-1, The Aerospace Corporation, El Segundo, California (30 June 1970).
25. K. F. Herzfeld and T. A. Litovitz, Absorption and Dispersion of Ultrasonic Waves, Academic Press, New York (1959).
26. D. L. Thompson, J. Chem. Phys. 57, 2589 (1972).
27. H. K. Shin, Chem. Phys. Lett. 10, 81 (1971); 11, 628 (1971); J. Chem. Phys. 59, 879 (1973).
28. H. K. Shin, J. Chem. Phys. 63, 2901 (1955).
29. H. K. Shin and Y. H. Kim, J. Chem. Phys. 64, 3634 (1976).

30. T. F. Deutsch, Appl. Phys. Lett. 11, 18 (1976).
31. O. D. Krogh and G. C. Pimentel, J. Chem. Phys. 67, 2993 (1977).
32. J. K. Hancock and A. W. Saunders, Jr., J. Chem. Phys. 65, 1275 (1976).
33. S. Ormonde, Rev. Modern Phys. 47, 193 (1975).



### THE IVAN A. GETTING LABORATORIES

The Laboratory Operations of The Aerospace Corporation is conducting experimental and theoretical investigations necessary for the evaluation and application of scientific advances to new military concepts and systems. Versatility and flexibility have been developed to a high degree by the laboratory personnel in dealing with the many problems encountered in the nation's rapidly developing space and missile systems. Expertise in the latest scientific developments is vital to the accomplishment of tasks related to these problems. The laboratories that contribute to this research are:

Aerophysics Laboratory: Launch and reentry aerodynamics, heat transfer, reentry physics, chemical kinetics, structural mechanics, flight dynamics, atmospheric pollution, and high-power gas lasers.

Chemistry and Physics Laboratory: Atmospheric reactions and atmospheric optics, chemical reactions in polluted atmospheres, chemical reactions of excited species in rocket plumes, chemical thermodynamics, plasma and laser-induced reactions, laser chemistry, propulsion chemistry, space vacuum and radiation effects on materials, lubrication and surface phenomena, photosensitive materials and sensors, high precision laser ranging, and the application of physics and chemistry to problems of law enforcement and biomedicine.

Electronics Research Laboratory: Electromagnetic theory, devices, and propagation phenomena, including plasma electromagnetics; quantum electronics, lasers, and electro-optics; communication sciences, applied electronics, semi-conducting, superconducting, and crystal device physics, optical and acoustical imaging; atmospheric pollution; millimeter wave and far-infrared technology.

Materials Sciences Laboratory: Development of new materials; metal matrix composites and new forms of carbon; test and evaluation of graphite and ceramics in reentry; spacecraft materials and electronic components in nuclear weapons environment; application of fracture mechanics to stress corrosion and fatigue-induced fractures in structural metals.

Space Sciences Laboratory: Atmospheric and ionospheric physics, radiation from the atmosphere, density and composition of the atmosphere, aurorae and airglow; magnetospheric physics, cosmic rays, generation and propagation of plasma waves in the magnetosphere; solar physics, studies of solar magnetic fields; space astronomy, x-ray astronomy; the effects of nuclear explosions, magnetic storms, and solar activity on the earth's atmosphere, ionosphere, and magnetosphere; the effects of optical, electromagnetic, and particulate radiations in space on space systems.

THE AEROSPACE CORPORATION  
El Segundo, California